

Maximum Power Point Tracking for Thermoelectric Generators with High Frequency Injection

Romina Rodriguez, Matthias Preindl, Ali Emadi, and James Cotton
McMaster Institute for Automotive Research and Technology (MacAUTO)
McMaster University, Hamilton, Ontario, Canada

Email: romina@mcmaster.ca, preindl@mcmaster.ca, emadi@mcmaster.ca, cottonjs@mcmaster.ca

Abstract—Thermoelectric Generators (TEG) can harvest a part of the thermal energy otherwise lost in the exhaust gases of vehicles and are combined with Maximum Power Point Tracking (MPPT) schemes to maximize the power output. This paper proposes a novel TEG MPPT scheme named High Frequency Injection (HFI) method. The method injects a high frequency voltage to the TEG and yields a power with a high frequency component. This component is demodulated and yields a signal proportional to the distance from the optimal operation point. The duty cycle setpoint is adjusted with a proportional-integral (PI) controller. The method is compared to the Perturb & Observe method using a drive cycle. Both show good results in terms of dynamic tracking of the optimal operation point. However, the HFI method is shown to be significantly more robust against sensor noise.

Index Terms—High Frequency Injection (HFI), Maximum Power Point Tracking (MPPT), Perturb & Observe, Thermoelectric Generator (TEG)

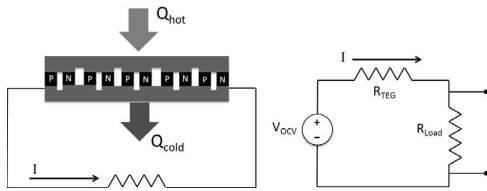


Fig. 1. Left:TEG schematic Right: TEG equivalent circuit

I. INTRODUCTION

A thermoelectric generator (TEG) is a solid state device that directly converts thermal energy to electrical energy when a temperature difference is applied across the TEG. Additional advantages of TEGs are their small size, reliability, low-maintenance cost and no moving parts (quiet operation). A schematic of a typical TEG is shown on the left in Figure 1 where heat flows through the hot-side and is dissipated in the cold-side while a portion of the thermal energy is converted to electricity. Due to the advantage of direct thermal to electrical energy conversion, TEGs are currently being investigated as a technology to recover waste heat from thermal processes to increase a system’s fuel efficiency. One application for TEGs is to recover thermal energy in the exhaust system of a vehicle.

Currently, vehicles with a gasoline engine lose about 40% (varies with drive cycle and driving conditions) of their fuel energy as waste heat in the exhaust gases. The consumption of the fuel energy of a conventional internal combustion engine

(ICE) vehicle is shown in Figure 2 [1]. As the fuel energy diagram shows, only about 15% of the fuel goes into driving the car while most of it is lost as thermal energy. The largest portion which is indicated as 40~70% energy is lost as heat through the cylinder head and the exhaust system. If this energy could be recovered and converted to useful energy then the total amount of fuel used by a vehicle could be reduced, thus increasing the efficiency of the vehicle.

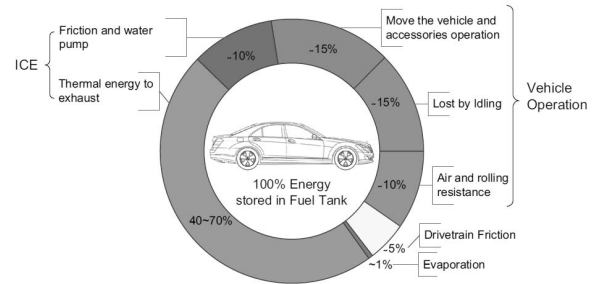


Fig. 2. Typical ICE car fuel consumption [1]

TEGs have only one Maximum Power Point (MPP) where a particular combination of voltage and current produces the highest output power for a given operating condition. As seen in the experimental work of [2], the voltage versus current curve is linear for a TEG and the power output is parabolic with only one maximum power point. The equivalent circuit for a TEG is shown on the right in Figure 1 and the voltage across the internal resistance and voltage across the load resistance is expressed as

$$V_{OCV} = V_{R_{TEG}} + V_{R_{Load}} \quad (1)$$

Since waste heat can be considered as a “free” source of energy, focus is on maximizing the power output of the TEG instead of maximizing efficiency. During a vehicle’s drive cycle, the exhaust temperature of the gases and thus the operating condition of the TEGs is varying. To optimize power output, the TEG should not charge a battery with a constant load voltage. The goal is to maximize the power output at the terminal of the TEG. To find the maximum power, start with

$$P = I^2 R_{Load} \quad (2)$$

The current is equal to the total voltage divided by the total resistance and since the TEG resistance and load resistance

are in series, these can be summed. (1) is plugged into (2) to get (3). The maximum power is now found by taking the derivative of P with respect to R_{Load} .

$$P = \left(\frac{V_{OCV}}{R_{TEG} + R_{Load}} \right)^2 R_{Load}. \quad (3)$$

The derivative of the power is described by

$$\frac{dP}{dR_{Load}} = \frac{-(V_{OCV})^2(R_{Load} - R_{TEG})}{(R_{Load} + R_{TEG})^3}, \quad (4)$$

and is equal to zero when a maximum occurs. The only way that the derivative will equal zero is if $(R_{Load} - R_{TEG}) = 0$ which means the maximum power output will occur when $R_{Load} = R_{TEG}$. Since the same current flows through the TEG resistance and the load resistance, the voltage drop across them is equal from $V = IR = IR_{TEG}$, and plugging this into (1), the maximum power is achieved when

$$V_{Load} = \frac{1}{2}V_{OCV}. \quad (5)$$

A. MPPT Algorithms

The most common MPPT schemes for TEGs in the literature are the Perturb & Observe (P&O), Incremental Conductance (INC), and the fractional voltage technique [3],[4],[5].

The P&O scheme works by tracking the measured output voltage and current, calculating the power output and stepping the terminal voltage in a particular direction. The voltage, current, and power are measured again and if the power is greater than the previously calculated power then the MPP will be reached by stepping the terminal voltage in the same direction. However, if the power is less than the previously calculated power then the MPP is reached by stepping in the opposite direction. Repeating this procedure over and over again will assure that the MPP is approached. However, there's no way for this MPPT scheme to arrive at the exact MPP and thus will always oscillate around the MPP but never stabilize on it.

The incremental conductance (INC) algorithm steps the voltage just like the P&O method but checks if $\frac{\Delta I}{\Delta V}$ is greater or less than $-\frac{I}{V}$. So instead of only looking at the power, it checks the rate of change of the current over the voltage compared to the instantaneous measurement. The advantage is that using this method, the MPP can be determined exactly. The simplest way to match the internal resistance of the TEG is to set the load voltage to half the open circuit voltage of the TEG. This is known as the fractional voltage technique. For this method to be implemented, a controller needs to disconnect the TEG from the converter to measure the open circuit voltage, however this results in some setbacks. When the TEG is disconnected, no current is flowing through (or generating power) so at reconnection a transient will occur. Also, the voltage produced by the TEG may change during operation due to the Peltier effect when current is flowing through the semiconductor junctions. This is why setting the load voltage to half the open circuit voltage may not be accurate.

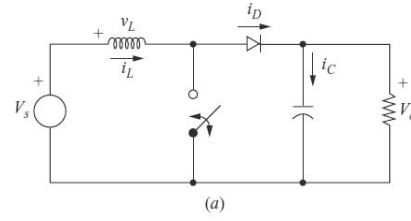


Fig. 3. Boost converter circuit [12]

One of the first who tracked the MPP by setting the terminal voltage to half the V_{OC} , open circuit voltage was [6]. In [7], the $V_{OC}/2$ scheme was also used but unlike previous authors, they did not measure the open circuit voltage by completely disconnecting the TEG from the converter. The input capacitors were disconnected by the microcontroller every 100 ms to allow for measurement of V_{OC} while the Buck converter was still connected to the load and the TEG. Researcher Yu used the P&O scheme to control the battery terminal voltage after the Cuk converter to account for converter losses, thus maximizing the power entering the battery [8].

This paper proposes the High-Frequency Injection (HFI) scheme based on drive systems and PV panels [9], [10], [11], which is referred to as ripple correlation control. HFI adds perturbation to the terminal voltage and evaluates the optimality of the operating point based on the high frequency response. In the following sections the most-commonly used P&O scheme and the HFI scheme are implemented to see if this MPPT can be used on TEGs and if it is effective in the presence of noise.

II. MODEL

A. TEG Model

A TEG can be modeled as a voltage source in series with a resistor, whose properties depend on the temperature difference across the TEG. The power will always be maximized when the load voltage on the TEG is half the TEG source voltage as described above in Section I. The simple TEG circuit was implemented in Simulink as shown by the left side of Figure 4.

B. Converter Model

A boost converter was chosen to control the terminal voltage of the TEG and achieve maximum power output. In this analysis, the boost converter is attached between the terminal leads of the TEG and the battery which is being charged by the TEG. A boost converter circuit is seen in Figure 3. The circuit operates with a switch and depending on whether it is on or off, the circuit will have different electrical characteristics. In the figure, V_s is the voltage that we are trying to control, in our case the load voltage (terminal voltage) of the TEG and V_o is the voltage of the battery. When the converter switch closes, current will travel through the least resistant path thus the voltage drop across the inductor, v_L , will be equal to V_s .

Since the inductor voltage drop is equal to V_s and thus positive, the current will increase linearly as described by

$$L \frac{di_L}{dt} = V. \quad (6)$$

When the switch is open, V_s will be distributed across the inductor and the output voltage, V_o , described by

$$V_s = v_L + V_o. \quad (7)$$

Therefore v_L is equal to $(V_s - V_o)$ when the switch is open and because the battery voltage is higher than V_s , it will be negative causing the conductor current to decrease. It is important to note here that the boost converter allows for a “boost” of V_s and thus V_s needs to be lower than V_o or the voltage of the battery.

Let the period for the switch opening and closing be equal to T , and let the time for the switch to be closed equal to DT where D is the duty cycle of the switch. Then the switch will be open for $T - DT = (1 - D)T$. The differential equation which describes the current of the inductor, (6), can be rewritten in terms of incremental differences as

$$L \frac{\Delta i_L}{\Delta t} = V. \quad (8)$$

The behavior of the inductor current can be written from (8) for the time when the switch is closed as

$$\frac{(\Delta i_L)_{ON}}{DT} = \frac{V_s}{L}, \quad (9)$$

ON describes the increasing current across the inductor when the switch is closed. The current equation for the inductor is also written for when the switch is open, where the inductor current is decreasing and is referred to by OFF in

$$\frac{(\Delta i_L)_{OFF}}{1 - DT} = \frac{V_s - V_o}{L}. \quad (10)$$

The magnitude of the change in the inductor current, Δi_L , is equal when the switch is closed and open. This can be described as $(\Delta i_L)_{ON} = -(\Delta i_L)_{OFF}$. Therefore the sum of the currents will be equal to zero and plugging in the values for the change in current from (9) and (10), the derivation of V_s as a function of duty cycle, (12), is seen in the steps

$$(\Delta i_L)_{ON} + (\Delta i_L)_{OFF} = 0 \quad (11a)$$

$$DT \frac{V_s}{L} + (1 - D)T \frac{(V_s - V_o)}{L} = 0 \quad (11b)$$

and yields

$$V_s = V_o(1 - D) \quad (12)$$

Next, is the analysis of the diode. There will be no current flowing across the diode when the switch is closed. However, when the switch is open the same current which flows through the inductor will flow through the diode so $i_D = i_L$. Integrating to calculate the average current of the diode over the

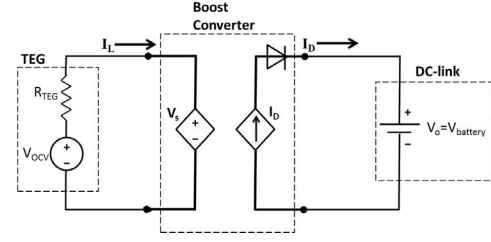


Fig. 4. Simplified converter and TEG model

period, (13a), we get (13b) knowing that the diode current is equal to the inductor current when the switch is open.

$$i_D = \frac{1}{T} \int_0^T i_D dt = \frac{1}{T} \int_0^{DT} i_D dt + \frac{1}{T} \int_{DT}^T i_D dt \quad (13a)$$

$$i_D = \frac{1}{T} \int_{DT}^T i_L dt. \quad (13b)$$

Since the magnitude of the inductor currents are equal, the following

$$i_L = \frac{1}{T} \int_0^T i_L dt = \frac{1}{(1 - D)T} \int_{DT}^T i_L dt, \quad (14)$$

describes the average current over the period.

Now combining (13b) and (14) we get

$$i_D = i_L(1 - D). \quad (15)$$

The analysis of the boost converter has resulted in two equations which describe the system as functions of the duty cycle of the switch. This allows a model of the converter in Simulink without having to model the switch which is advantageous because a high-frequency switch takes a lot of CPU power. Thus attaching the converter between the TEG and the battery, the system can be modeled as Figure 4, where the dashed lines show the boost converter which has been reduced to a voltage source and a current source modeled by (15) and (12).

From discussion in the introduction, the maximum power will be achieved when the load voltage of the TEG is equal to half the open circuit voltage of the TEG. Using the variables from Figure 4, it means we want V_s to be $0.5V_{OCV}$.

III. OPTIMIZATION SCHEMES

A. Perturb & Observe

The model created for the P&O scheme is shown in Figure 5. The battery voltage was set to 12V and this is used throughout all of this paper's analysis. To find the optimal operating duty cycle, the change in power is calculated from the previous two time steps. If the change in power is positive, then (16) is used to step D in the same direction and if the change in power is negative then (17) is used since D needs to be stepped in the opposite direction. ΔD is defined as the change in duty cycle from the previous two time steps i.e. $\Delta D = D_{old,old} - D_{old}$. The sign of ΔD is used since the initial operating duty cycle could be on the far right end of power

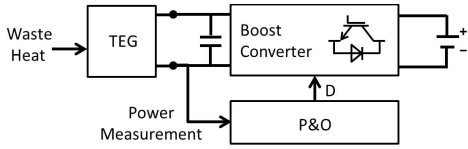


Fig. 5. Model for P&O scheme

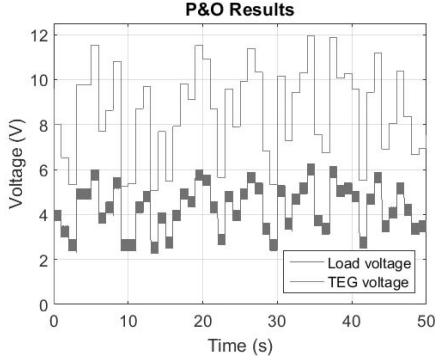


Fig. 6. P&O MPPT scheme

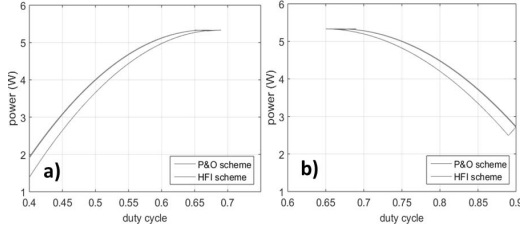


Fig. 7. P&O scheme, HFI scheme a) initial duty cycle: 0.4 b) initial duty cycle: 0.9

versus current curve and we would need to go backwards to get to the correct duty cycle. δd is the size of the step that is taken to change the duty cycle at the next time step and was chosen to be 0.01 here.

$$D = D_{old} + \delta_d \text{sign}(\Delta D) \quad (16)$$

$$D = D_{old} - \delta_d \text{sign}(\Delta D) \quad (17)$$

The results for the P&O scheme are shown in Figure 6, where the TEG voltage versus time is an input to the Simulink model and the load voltage is the output from the model showing the tracking of $0.5V_{OCV}$. As can be observed, the scheme works well and the load voltage is always half the TEG voltage which means that maximum power is achieved. To test if the scheme was accurately tracking the MPP, the TEG voltage was set to a constant of 8.0V and the model was initialized with a duty cycle of 0.4 and then another run was done with the duty cycle of 0.9 (Figure 7). This was done to verify accurate tracking of the MPP regardless of the initial duty cycle guess.

B. High-Frequency Injection

The high-frequency injection (HFI) scheme works by injecting a sine (high frequency) signal into the duty cycle of

the switch and from the measured power, an optimal duty cycle can be estimated. A Simulink model was created for this scheme which uses the previously described converter and TEG model but has extra components as shown in Figure 8 where a PI controller, high-pass and low-pass filter have been added. To understand how a sine signal injection can achieve MPPT, begin with the power output for the load voltage (terminal voltage) of the TEG,

$$P = IV = I_L V_s. \quad (18)$$

Then rewrite the equation with only known values (D , V_{OCV} , V_o), plug in (12) and (15) and simplify to get

$$P = I_L V_o (1 - D) \quad (19a)$$

$$= \frac{V_{OCV} V_o - V_{OCV} V_o D - V_o^2 + 2V_o^2 D - V_o^2 D^2}{R_{TEG}} \quad (19b)$$

Now a sine signal with angular frequency ω and amplitude A will be injected into the model so the duty cycle becomes, $d = D + A \sin(\omega t)$. This duty cycle is plugged back into the power equation, (18), and the derivation is the same as (18) through (19b) except d is the new duty cycle. The final answer is shown below where p is the power calculated from the injected signal:

$$\begin{aligned} p &= I_L V_o (1 - d) \\ &= \frac{V_{OCV} V_o - V_{OCV} V_o D - V_o^2 + 2V_o^2 D - V_o^2 D^2}{R_{TEG}} \\ &\quad + \frac{A \sin(\omega t) (2V_o^2 - 2DV_o^2 - V_{OCV} V_o)}{R_{TEG}} \\ &\quad - \frac{A^2 \sin^2(\omega t) V_o^2}{R_{TEG}}. \end{aligned} \quad (20)$$

Looking at (20), it can be rewritten as

$$p = P + \frac{A \sin(\omega t) [V_o (2V_s - V_{OCV})]}{R_{TEG}} - \frac{A^2 \sin^2(\omega t) V_o^2}{R_{TEG}} \quad (21)$$

by noting that the first term is the power with duty cycle D and the second term is a function of $(2V_s - V_{OCV})$, from (12). This provides interesting insight because to maximize power, we want the load voltage, or V_s , to be half of V_{OCV} (the TEG voltage) ie. $V_s = \frac{1}{2} V_{OCV}$ and looking at the second term of (21), this relationship pops up.

Let's further explore this by looking at only the high frequency terms which are the second and third term of (21). Since P is a low frequency term (doesn't have a sine term), a high-pass filter is used on p so that we now only have the last two terms of (21). However since the last term is a \sin^2 function, the high-pass filter will extract an offset since this function has an average value. Let's call this offset, or average value, C , where it is defined by

$$C = \frac{1}{\omega t} \int_0^{\omega t} \frac{A^2 \sin^2(\omega t) V_o^2}{R_{TEG}} d(\omega t) = \frac{A^2 V_o^2}{2R_{TEG}}. \quad (22)$$

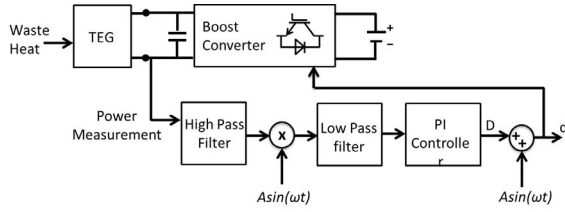


Fig. 8. Simulink model for HFI scheme

Now (21) can be rewritten after a high-pass filter has been applied to p as p_{hpf} described by

$$\begin{aligned}
 p_{hpf} &= p_1 + p_2 + C \\
 p_1 &= \frac{Asin(\omega t)V_o(2V_s - V_{OCV})}{R_{TEG}} \\
 p_2 &= -\frac{A^2 sin^2(\omega t)V_o^2}{R_{TEG}}
 \end{aligned} \quad (23)$$

To see if something useful can be extracted from $(2V_s - V_{OCV})$, multiply p_{hpf} by $Asin(\omega t)$ to get p_{sin}

$$p_{sin} = Asin(\omega t)p_1 + Asin(\omega t)p_2 + Asin(\omega t)C, \quad (24)$$

and apply a low pass filter which will result in an offset, P_{OF} , of p_{sin} defined by

$$P_{OF} = \frac{1}{\omega t} \int_0^{\omega t} p_{sin} d(\omega t). \quad (25)$$

By evaluating the average value, (25), P_{OF} is reduced to

$$P_{OF} = \frac{1}{\omega t} \int_0^{\omega t} Asin(\omega t)p_1 d(\omega t) = \frac{A^2 V_o(2V_s - V_{OCV})}{2R_{TEG}}. \quad (26)$$

since the average value of sin^3 and sin is always zero over an entire number of periods. The offset can be negative or zero depending only on the sign of $(2V_s - V_{OCV})$ because the constants $\frac{A^2 V_o}{R_{TEG}}$ are always positive.

Three different cases now exist. *Case 1:* $V_s = V_{OCV}/2$, which tells us that we are operating at maximum power output and would make the offset equal to zero. *Case 2:* $V_s > V_{OCV}/2$ which tells us that the load voltage is higher than $V_{OCV}/2$ and results in a positive offset. *Case 3:* $V_s < V_{OCV}/2$ which tells us that the load voltage is lower than $V_{OCV}/2$ and results in a negative offset. The error or the difference from what the duty cycle should be is proportional to the offset, P_{OF} . Thus this error can be used as feedback for a proportional integral controller to correct the duty cycle D with KP_{OF} added, where K is a gain value determined through trial and error.

The perturbation or injection frequency is chosen such that it can be resolved well in presence of the power electronic sampling times, e.g. one order of magnitude slower. The high and low pass filter are designed to operate on signals at injection frequency. Hence their bandwidth is chosen at least one order of magnitude lower than the injection frequency. In this research, the power electronic sampling frequency is 100kHz, the injection frequency is 1kHz, the bandwidth of the

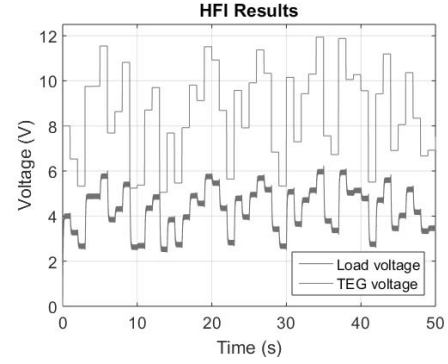


Fig. 9. HFI MPPT scheme

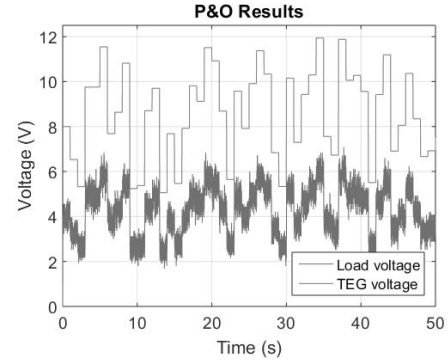


Fig. 10. P&O scheme results in the presence of measurement noise

high pass filter is 100Hz, and the bandwidth of the low pass filter is 10Hz.

The HFI results for the same TEG voltage used in the P&O scheme are in Figure 9. The scheme works correctly just as the P&O scheme.

The same verification of MPP tracking regardless of initial duty cycle was conducted for this scheme as in the P&O scheme, described in section III-A. The MPP is seen tracked by the high-frequency injection scheme in Figure 7 regardless of the starting point.

IV. COMPARISON OF METHODS

This section will focus on comparing the two MPPT methods. Since both worked well for the TEG voltage input, white noise was introduced to the model to see the effect on tracking. White noise is added to test the robustness of the MPPT schemes. A 1% noise has been added to the voltage signal to account for actuation uncertainties and a 1% noise was added to the current measurement to account for measurement noise. The results for tracking voltage with noise measurement is seen in Figure 10 for the P&O MPPT scheme and in Figure 11 for the HFI scheme.

It's observed, that the P&O scheme fluctuates significantly when noise is introduced while the HFI scheme displays almost no change in tracking. This can be better observed when noise is added to track a constant voltage in Figure 12. Finally the total energy produced from each scheme was

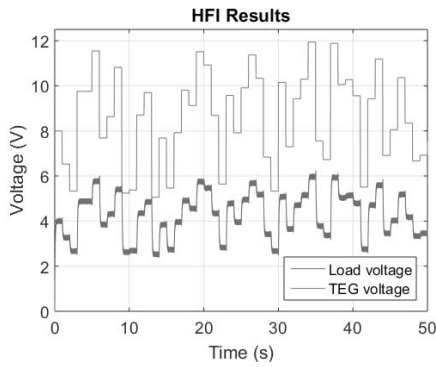


Fig. 11. HFI scheme results in the presence of measurement noise

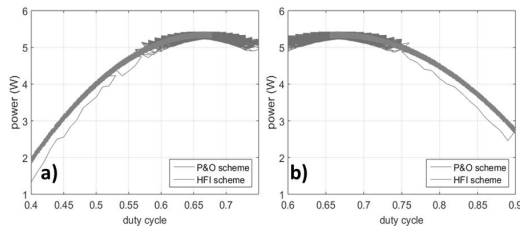


Fig. 12. MPPT schemes compared when noise is added for initial duty guess of a) 0.4 and b) 0.9

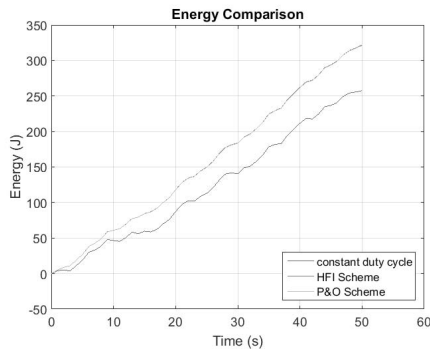


Fig. 13. The total energy produced by the HFI scheme, P&O scheme and a fixed duty cycle of 0.5

found by integrating the power over the simulation time and compared to a converter which used a fixed duty cycle of 0.5. The total energy produced by the HFI scheme was 321.76 Joules, 321.2 Joules for the P&O scheme and 257.45 Joules for using a fixed duty cycle of 0.5 throughout operation.

The total energy values are seen in Figure 13. As can be seen, not utilizing a MPPT scheme while a TEG is used in a vehicle produces a loss of almost 20% from the total energy that could be captured. The difference between the energy calculated from the HFI scheme and the P&O scheme is about 0.2%. However it is noted that, the large high frequency components in the P&O results in a larger current ripple. This ripple is expected to yield higher losses in the power circuits in particular inductors but is not considered in this research.

V. CONCLUSION

This research proposes the High-Frequency Injection (HFI) scheme for Maximum Power Point Tracking (MPPT) of thermoelectric generators (TEG). It is compared to the frequently-used Perturb & Observe (P&O) scheme. Both schemes tracked the MPP well in absence of measurement noise. In presence of noise, the HFI scheme is able to track the MPP point significantly better than the P&O using a similar level of perturbation. However, as the MPP point is a flat optimum the energy harvested by both schemes is comparable with modest advantages for HFI. The schemes are also compared to operation at constant terminal voltage confirming the waste heat recovery advantages of MPPT.

ACKNOWLEDGMENT

This research was undertaken, in part, thanks to funding from the Canada Excellence Research Chairs Program.

REFERENCES

- [1] S. F. Tie and C. W. Tan, "A review of energy sources and energy management system in electric vehicles," *Renewable and Sustainable Energy Reviews*, vol. 20, pp. 82–102, 2013. [Online]. Available: <http://dx.doi.org/10.1016/j.rser.2012.11.077>
- [2] A. Montecucco, S. Member, A. R. Knox, and S. Member, "Maximum Power Point Tracking Converter Based on the Open-Circuit Voltage Method for Thermoelectric Generators," *IEEE Transactions on Power Electronics*, vol. 30, no. 2, pp. 1–12, 2014.
- [3] K. I. M. Bunther, B. U. N. Long, G. Christophe, D. Bruno, M. Pascal, and A. M. Model, "Modeling and tuning of MPPT Controllers for a Thermoelectric Generator," in *First International Conference on Green Energy ICGE 2014*, vol. 2, 2014, pp. 220–226.
- [4] H. Park, M. Sim, and S. Kim, "Achieving Maximum Power from Thermoelectric Generators with Maximum-Power-Point-Tracking Circuits Composed of a Boost-Cascaded-with-Buck Converter," *Journal of Electronic Materials*, 2015.
- [5] R. Y. Kim and J. S. Lai, "Aggregated modeling and control of a boost-buck cascade converter for maximum power point tracking of a thermoelectric generator," *Conference Proceedings - IEEE Applied Power Electronics Conference and Exposition - APEC*, pp. 1754–1760, 2008.
- [6] H. Nagayoshi and T. Kajikawa, "Mismatch Power Loss Reduction on Thermoelectric Generator Systems Using Maximum Power Point Trackers," *2006 25th International Conference on Thermoelectrics*, pp. 0–3, 2006.
- [7] A. Montecucco, J. Siviter, and A. R. Knox, "Simple, fast and accurate maximum power point tracking converter for thermoelectric generators," in *Energy Conversion Congress and Exposition (ECCE), 2012 IEEE*, 2012, pp. 2777–2783.
- [8] C. Yu and K. Chau, "Thermoelectric automotive waste heat energy recovery using maximum power point tracking," *Energy Conversion and Management*, vol. 50, no. 6, pp. 1506–1512, Jun. 2009.
- [9] P. Krein, "Ripple correlation control, with some applications," *ISCAS'99. Proceedings of the 1999 IEEE International Symposium on Circuits and Systems VLSI (Cat. No.99CH36349)*, vol. 5, pp. 283–286, 1999.
- [10] G. Spiazzi, S. Buso, and P. Mattavelli, "Analysis of MPPT algorithms for photovoltaic panels based on ripple correlation techniques in presence of parasitic components," *2009 Brazilian Power Electronics Conference, COBEP2009*, pp. 88–95, 2009.
- [11] T. ESRAM, S. Member, J. W. Kimball, S. Member, P. T. Krein, P. L. Chapman, S. Member, P. Midya, and S. Member, "Dynamic Maximum Power Point Tracking of Photovoltaic Arrays Using Ripple Correlation Control.pdf," vol. 21, no. 5, pp. 1282–1291, 2006.
- [12] Daniel W. Hart, *Power Electronics*. McGraw-Hill, 2011.